Tropomyosin Requires an Intact N-Terminal Coiled Coil to Interact with Tropomodulin

Norma J. Greenfield* and Velia M. Fowler†

*University of Medicine and Dentistry of New Jersey—Robert Wood Johnson Medical School, Piscataway, New Jersey 08854-5635 USA; and †The Scripps Research Institute, La Jolla, California 92037 USA

ABSTRACT Tropomodulins (Tmods) are tropomyosin (TM) binding proteins that bind to the pointed end of actin filaments and modulate thin filament dynamics. They bind to the N termini of both "long" TMs (with the N terminus encoded by exon 1a of the α-TM gene) and "short" nonmuscle TMs (with the N terminus encoded by exon 1b). In this present study, circular dichroism was used to study the interaction of two designed chimeric proteins, AcTM1aZip and AcTM1bZip, containing the N terminus of a long or a short TM, respectively, with protein fragments containing residues 1 to 130 of erythrocyte or skeletal muscle Tmod. The binding of either TMZip causes similar conformational changes in both Tmod fragments promoting increases in both α-helix and β-structure, although they differ in binding affinity. The circular dichroism changes in the Tmod upon binding and modeling of the Tmod sequences suggest that the interface between TM and Tmod includes a three- or four-stranded coiled coil. An intact coiled coil at the N terminus of the TMs is essential for Tmod binding, as modifications that disrupt the N-terminal helix, such as removal of the N-terminal acetyl group from AcTM1aZip or striated muscle α-TM, or introduction of a mutation that causes nemaline myopathy, Met-8-Arg, into AcTM1aZip destroyed Tmod binding.

INTRODUCTION

The actin filament network immediately under the plasma membrane in regions of cellular protrusion consists of a dendritic network of short, branched filaments. In contrast, the actin filaments deeper in the cortex, in stress fibers and microvilli, as well as those in muscle sarcomeres are much longer and rarely branched (Small, 1995; Bailly et al., 1999; Svitkina and Borisy, 1999). Actin binding proteins regulate actin filament dynamics spatially and temporally by affecting nucleation of polymerization, the kinetics of monomer addition and loss at the filament ends and the severing of the filament.

Factors that stabilize new filaments by protecting them from pointed end depolymerization or from severing can result in stable, unbranched filaments. For example, tropomyosin (TM), a coiled-coil protein that binds along the sides of actin filaments, inhibits the rate of depolymerization from the pointed end, without affecting elongation (Broschat et al., 1989; Broschat, 1990). Elongation of TM-actin filaments from the pointed end can be blocked by tropomodulin (Tmod), an actin filament pointed end-capping protein that also binds TM (Weber et al., 1994, 1999). In striated muscle, Tmod is specifically associated with actin and TM at the thin filament pointed ends where it regulates thin filament length in vivo (Gregorio et al., 1995; Gregorio and Fowler, 1995; Sussman et al., 1998; Littlefield et al., 2001). Tropomyosin also inhibits the ability of actin filaments to act as secondary activators of nucleation in the formation of filament branches by the activated Arp 2/3 complex (Blanchoin et al., 2001) and protects actin filaments from severing proteins such as actin-depolymerizing factor/cofilin (Bamburg et al., 1999).

Tropomyosin and tropomodulin both belong to multigene families that are expressed widely in eukaryotic cells. The TMs belong to two major classes: "long" ~285 residue TMs, which are expressed in muscle and nonmuscle cells and "short" ~247 residue isoforms, which are found in nonmuscle cells. In the α-TM gene (human *TPM1*) alternate promotor selection results in gene products that express exon 1a and 2 (residues 1–80) in long isoforms or exon 1b (residues 1–43) in short isoforms (Helfman et al., 1986; Lin et al., 1988). Long and short TM isoforms share common functions including actin binding, regulation with myosin, stabilization and stiffening of the actin filament (for reviews, see Tobacman, 1996; Lin et al., 1997), and inhibition of the Arp 2/3 complex nucleated branching (Blanchoin et al., 2001), although there are some isoform differences (Novy et al., 1993; Fanning et al., 1994; Moraczewska et al., 1999). The exon 1a encoded sequence is highly conserved throughout phylogeny and is essential for actin binding of long TM isoforms (Cho et al., 1990; Moraczewska et al., 2000). Modifications such as lack of N-terminal acetylation or introduction of a nemaline myopathy-causing mutation, Met-8-Arg, severely reduce the actin affinity of skeletal muscle α-TM (Heald and Hitchcock-DeGregori, 1988; Urbancikova and Hitchcock-DeGregori, 1994).

Tropomodulin isoforms are also widely expressed (Fowler and Conley, 1999). Tropomodulin was originally isolated from human erythrocytes as a tropomyosin-binding protein (Fowler, 1987, 1990). Two major tropomodulin isoforms are E-tropomodulin (E-Tmod, Tmod1) and Sk-tropomodulin (Sk-Tmod, Tmod4) (Almenar-Queralt et al., 1999; Cox and Zoghbi, 2000; Conley et al., 2001). E- and Sk-Tmods differ in their tissue distribution: in mammals, E-Tmod is the predominant isoform in heart and slow skeletal muscle as well as in erythrocytes,

Submitted October 24, 2001, and accepted for publication February 12, 2002.

Address reprint requests to Norma J. Greenfield, UMDNJ-Robert Wood Johnson Medical School, 675 Hoes Lane, Piscataway, NJ 08854-5635. Tel.: 732-235-5791; Fax: 732-235-4029; E-mail: greenfie@rwja.umdnj.edu.

0006-3495/02/05/2580/12 $2.00

whereas Sk-Tmod is exclusively expressed in skeletal muscle (Conley et al., 2001). In chickens, Sk-Tmod is the predominant isoform in fast skeletal muscle and in erythrocytes, whereas E-Tmod is predominant in the heart and slow skeletal muscle fibers. In chicken skeletal muscle fibers that coexpress both Sk- and E-Tmods, the Tmods are recruited to different actin filament-containing cytoskeletal structures within the cell: myofibrils and costameres, respectively (Almenar-Queralt et al., 1999). These results suggest that vertebrates have different Tmod isoforms that play distinct roles in vivo.

The Tmods have distinct TM and actin binding domains (Babcock and Fowler, 1994; Gregorio et al., 1995) with the binding site for TM being in the N-terminal half of Tmod. Tmod binds to the N terminus of TM (Sung and Lin, 1994). Recently mutagenesis studies mapped the binding for recombinant human E-Tmod to the first heptad of the coiled-coil region (residues 6–13) of human tropomyosin hTM5, a product of the *TPM4* gene (Vera et al., 2000).

In this present study, circular dichroism (CD) was used to study the structural changes that accompany Tmod-TM interaction and the specificity of the interaction among different isoforms of TM and Tmod. We used recombinant constructs of full-length E-Tmod and N-terminal fragments of E- and Sk-Tmods (E-Tmod$_{1–130}$ and Sk-Tmod$_{1–130}$) that contain the TM binding domain and measured their interactions with AcTM1aZip and AcTM1bZip, two designed chimeric proteins previously used for structural studies of the N terminus of TM (Greenfield et al., 1998, 2001). AcTM1aZip and AcTM1bZip contain the first 14 and 19 residues of long and short rat α-TMs encoded by exon 1a and exon 1b, respectively, and the 18 C-terminal residues of the leucine zipper domain of the yeast transcription factor, GCN4 (Landschulz et al., 1988). The TMZip chimeras, although very short, exhibit many of the functions of full length TMs. For example, AcTM1aZip binds to peptides containing the C terminus of striated TM to form a 1:1 complex. This binary complex binds tightly to a protein fragment containing the TM binding domain of Troponin T (TnT) to form a ternary complex with 1:1:1 stoichiometry (Palm et al., 2001).

We found that the TMZip chimeric proteins bind to full length E-Tmod and to fragments containing the N-terminal 130 residues of both Sk- and E-Tmod and that there are isoform specific differences in binding affinity. In addition, our results give insight into the structure of the Tmod-TM complexes.

MATERIALS AND METHODS

Materials

AcTM1aZip, GlyTM1aZip, Tm1aZip, and AcTM1bZip were synthesized by SynPep (Dublin, CA) and AcTM1aZipM8R was synthesized by the W.M. Keck Biotechnology Resource Center (New Haven, CT). All the proteins were greater than 95% pure when analyzed by reverse-phase high-performance liquid chromatography on a C-18, 5 μ, 40 $\times$ 100 mm column. The molecular masses determined by electrospray mass spectroscopy (expected versus found) were the following, respectively: AcTM1aZip, 3886.0 vs. 3887.0; TM1aZip, 3842.2 vs. 3843.0; GlyTm1aZip, 3900.7 vs. 3900.0; AcTM1bZip, 4307.9 vs. 4308.0; AcTM1aZipM8R, 3912.0 vs. 3910.6. GlyTM1bZip was expressed in *Escherichia coli* as described previously (Greenfield et al., 2001).

Full-length E-Tmod (359 residues) and fragments containing residues 1 to 130 of Sk-Tmod and E-Tmod were expressed as fusion proteins with glutathione S-transferase in *E. coli* and purified as previously described by affinity chromatography on glutathione-sepharose followed by thrombin cleavage to remove the glutathione S-transferase moiety, leaving an N-terminal extension of 13 to 15 residues (Babcock and Fowler, 1994). The full length protein and fragments were purified to homogeneity on sequential ResourceQ and MonoQ columns by fast-protein liquid chromatography (Pharmacia, Uppsala, Sweden) giving yields of ~2 mg/L of bacterial culture for E-Tmod$_{1–130}$ and ~8 mg/L for Sk-Tmod$_{1–130}$. The molecular masses were 16,257 Da for E-Tmod$_{1–130}$, 16,238 Da for Sk-Tmod$_{1–130}$, and 41,542 Da for E-Tmod.

Circular dichroism measurements

CD measurements were made using an Aviv model 62 DS spectropolarimeter as previously described (Greenfield and Hitchcock-DeGregori, 1995; Greenfield et al., 1998). All the TMZips (1–2 mg) were dissolved in 0.5 mL of 100 mM NaCl, 10 mM sodium phosphate, pH 6.5 and then desalted on NAP5 columns (Pharmacia Biotech, Uppsala, Sweden) equilibrated with the same buffer. The protein concentrations of the TMZip stock solutions (two polypeptide chains/molecule) were determined from measurements of their difference spectra in 6 M guanidine-HCl between pH 12.5 and pH 6.0 using a molar extinction coefficient of 4714 M^{-1} cm^{-1} at 294 nm (Edelhoch, 1967; Fasman, 1989). The protein concentrations of the Tmod stock solutions were determined using the following molar extinction coefficients at 280 nm: E-Tmod$_{1–359}$, 14650 M^{-1} cm^{-1}; E-Tmod$_{1–130}$, 8250 M^{-1} cm^{-1}; Sk-Tmod1–130, 2560 M^{-1} cm^{-1}. The CD spectra were analyzed for secondary structure content using three different methods: the self-consistent singular value decomposition method of Sreerama and Woody (1994), CDNN, a neural network analysis program (Bohm et al., 1992), and a constrained least squares fit analysis program (Perczel et al., 1992) using a polypeptide reference set (Brahms and Brahms, 1980).

Thermodynamics of folding

The enthalpy and entropy of folding of the TM1aZip and TM1bZip proteins were determined from the change in ellipticity as a function of temperature as described previously (Greenfield et al., 1998). To determine the enthalpy and entropy of folding of the TMZip-Tmod complexes, the CD of the complex of the TMZips with TMod as a function of temperature were fit to the Gibbs-Helmholtz equation for a two-state transition assuming that 1 mol of a folded complex dissociates to give 2 mol of unfolded monomeric TMZip and 1 mol of the unfolded Tmod fragment. The equations used are similar to those used to describe the unfolding of homotrimers (Engel et al., 1977; Marky and Breslauer, 1987). In these equations α is the fraction folded, k is the binding constant, C is the concentration of the TMZip-Tmod complex, T is the temperature, T_M is the temperature in which $\alpha = 0.5$, and R is

the gas constant, 1.987 cal/mol. The data were fit using the following equations:

$$k = \text{trimer/monomers} = C\alpha/[(2C(1-\alpha))^2(C(1-\alpha))] \quad (1)$$

$$\Delta G = -nRT \ln k = \Delta H - T\Delta S \quad (2)$$

Combining and rearranging terms one obtains

$$k = \exp((\Delta H/RT)(T/T_M - 1)) - \ln(C^2)) \quad (3)$$

solving Eq. (1), which is a cubic, for α in terms of k

$$Q = -1/(12C^2k) \quad (4)$$

$$S = -1/(8C^2k) \quad (5)$$

$$A = -(S + \text{sqrt}(S^2 - Q^3))^{(1/3)} \quad (6)$$

$$B = Q/A \quad (7)$$

$$\alpha = 1 - (A + B) \quad (8)$$

The observed ellipticity at any temperature is directly proportional to α

$$\theta_{obs} = (\theta_F - \theta_U)\alpha + \theta_U \quad (9)$$

in which θ_F is the ellipticity of the folded trimer and θ_U is the sum of the ellipticity of the monomers. Initial values of ΔH, T_M, θ_F, and θ_U were estimated, and θ_{obs} was fit to the raw data by nonlinear least squares curve fitting to determine their best fit values using the Levenberg-Marquardt algorithm (Marquardt, 1963) implemented in SigmaPlot (SPSS Science, Chicago, IL). The entropy of folding, ΔS, was evaluated at the T_M apparent in which $\alpha = 0.5$ using Eqs. 1 and 2, and it was assumed that ΔS was independent of temperature. In all of these calculations the change in heat capacity upon unfolding was assumed to be zero. The unfolding and folding of the TMZip and TMZip-Tmod$_{1-130}$ complexes were all reversible.

Binding constants

Binding constants for E-Tmod$_{1-130}$ and Sk-Tmod$_{1-130}$ for AcTM1aZip and AcTM1bZip were estimated in two ways. 1) The free energy of folding of the TMZip two-chained coiled coils and the three chained Tmod-TMZip complexes at 30°C (303.15 K) were determined from their enthalpies (ΔH) and entropies (ΔS) of folding (determined above) using the relationship $\Delta G = \Delta H - T\Delta S$, in which ΔH and ΔS were assumed to be independent of temperature and T is the absolute temperature. It was assumed that all of the difference in the free energy of folding of the TMZip-Tmod complex and free TMZip were due to the binding and that the dissociation constant for the Tmod-TM fragment complexes, $k_d = 1/\exp(-\Delta\Delta G/nRT)$. The unbound Tmod fragments did not change conformation between 0 and 70°C and their contributions to the free energy change were assumed to be zero. 2) The TMZip chimeras were directly titrated with the Tmod fragments by observing the increase in negative ellipticity at 222 nm when the Tmod fragments were added to the TMZips compared with the Tmod fragments alone added to buffer. The TMZips, 0.5 mL, 10 μM, in 100 mM NaCl, 10 mM sodium phosphate, pH 6.5, at 30°C were titrated with concentrated solutions of Sk- or E-Tmod$_{1-130}$. The ellipticity change was corrected for dilution (0.5–0.7 mL), but it was assumed that the concentration of TMZip and total volume did not change during the titration for the purposes of estimating the binding constants. The ellipticity changes were used to determine the binding constant and number of binding sites as described by Engel (1974) using the equation:

$$\theta_{obs} = \theta_{Max}((1 + (kC/n) + kP)/(2kP) - \text{sqrt}(((1 + (kC/n) + kP)/(2kP))^2 - C/(nP)))$$

in which k is the binding constant, P is the protein concentration of the TMZip fragments, C is the total concentration of the Tmod fragment added, n is the number of binding sites, θ_{obs} is the observed ellipticity change at any concentration of Tmod, and θ_{max} is the ellipticity change when all of the TMZip binds Tmod. Initial values of θ_{Max}, k, and n were estimated and the raw data were fit to the equation to determine their final values using the Levenberg-Marquardt algorithm (Marquardt, 1963) implemented in SigmaPlot (SPSS Science).

RESULTS

The N termini of the TMs have long been known to be critical determinants of its interactions with the actin thin filament and regulation of contraction. In this present study we found that the extreme N-terminal coiled-coil domains of the TMs also are essential and specific for their interactions with Tmod. Circular dichroism was first used to estimate the secondary structure of the Tmod fragments and to elucidate the structural changes that occurred upon complex formation with the TM chimeric proteins. The changes in CD as a function of temperature were used to determine the binding constants of the TM-Tmod complexes and to investigate the effects of modifications that altered the coiled-coil content of the free TM proteins on their ability to interact with the Tmods. The sequences and alignments of the TM chimeras containing the N termini of the long and short TMs (TM1aZip and TM1bZip) are given in Fig. 1 and those of the Sk-and E-Tmod$_{1-130}$ fragments are given in Fig. 2. In the following we illustrate representative data in the figures and present the results for all the proteins and their interactions (see Tables 2 and 3).

Secondary structures of full length Tmod, the Tmod fragments, and the TM chimeras

The secondary structures of E-Tmod$_{1-359}$ and E-Tmod$_{1-130}$ and Sk-Tmod$_{1-130}$, were estimated using circular dichroism spectroscopy. Fig. 3 *A* shows CD spectra of E-Tmod$_{1-359}$ at 0 and 70°C. Three different procedures used to estimate the secondary structure (see Materials and Methods) gave results in good agreement with each other: 22 ± 2% α-helix, 26 ± 3% β-sheet, with the remainder consisting of β-turns, extended poly-L-proline (PP2) type structure and regions without defined secondary structure. When the protein was heated from 0 to 70°C, there was little change in ellipticity at 222 nm, but the spectral maximum shifted to 218 nm, suggesting that the protein aggregated at high temperatures. The CD spectra of E-Tmod$_{1-130}$ and Sk-Tmod$_{1-130}$ were similar to each other (Fig. 3 *B*), and were characteristic of unfolded polypeptides with some transient residual α-helical content (20%–30%)

Alignment of TMZip Sequences

Source=α-TM																			
								1				5				10			
AcTM1aZip						Ac	M	D	A	I	K	K	K	M	Q	M	L	K	L	D
		1				5					10					15				
AcTM1bZip	Ac	A	G	S	S	S	L	E	A	V	R	R	K	I	R	S	L	Q	E	Q
Heptad repeat							*a*			*d*				*a*			*d*			
Source=GCN4																			
		15					20					25					30			
AcTM1aZip		N	Y	H	L	E	N	E	V	A	R	L	K	K	L	V	G	E	R	
		20					25					30					35			
AcTM1bZip		N	Y	H	L	E	N	E	V	A	R	L	K	K	L	V	G	E	R	
Heptad repeat		*a*			*d*				*a*			*d*				*a*				

FIGURE 1 Sequence of tropomyosin chimeric proteins containing the N termini of rabbit long α-TMs encoded by exon 1a, TM1aZip, and rat short α-TMs encoded by exon 1b. The sequences of TM1aZip (residues 1–14) are identical to those of rabbit striated muscle α-tropomyosin (Stone and Smillie, 1978) and the sequence of residues 1 to 19 of TM1bZip are identical to those of rat short tropomyosin (Helfman et al., 1986). Residues 15 to 32 of TM1aZip and 20 to 37 of TM1bZip corresponds to the last 18 C-terminal residues (264–281) of the yeast transcription factor GCN4 (Landschulz et al., 1988). The residues that are coiled coil are labeled with the residue position of the heptad repeats in italics. In GlyTM1aZip and GlyTM1bZip a glycine residue replaces the N-terminal acetyl group.

(Greenfield and Hitchcock-DeGregori, 1993). These CD spectra did not change between 0 and 70°C (not shown), also indicating that they were essentially unfolded. Similar results for a shorter 90-residue N-terminal fragment of E-Tmod have been reported previously (Kostyukova et al., 2000). The CD spectra of AcTM1aZip and AcTM1bZip were characteristic of

Alignment of Sk- and E-Tropomodulin$_{1\text{-}130}$ Sequences

E	(G	S	P	G	I	S	G	G	G	G		G	I	L)													
Sk	(G	S	P	G	I	S	G	G	G	G		G	I	L	D	S)											
E	M	-	**S**	**Y**	**R**	K	**E**	**L**	**E**	**K**		**Y**	**R**	**D**	L	**D**	**E**	**D**	**K**	**I**	**L**	19					
SK	M	T	**S**	**Y**	**R**	Q	**E**	**L**	**E**	**K**		**Y**	**R**	**D**	I	**D**	**E**	**D**	**K**	**I**	**L**	20					
E	G	A	**L**	T	E	**E**	**E**	**L**	R	K		**L**	E	N	**E**	**L**	E	**E**	L	**D**	**P**	39					
Sk	Q	E	**L**	S	A	**E**	**E**	**L**	E	Q		**L**	D	T	**E**	**L**	L	**E**	M	**D**	**P**	40					
					e	*f*	*g*	*a*	*b*	*c*		*d*	*e*	*f*	*g*	*a*	*b*	*c*	*d*	*e*							
E	D	**N**	A	**L**	**L**	**P**	**A**	**G**	**L**	**R**		**Q**	**R**	**D**	**Q**	**T**	**Q**	**K**	P	**P**	**T**	59					
SK	E	**N**	V	**L**	**L**	**P**	**A**	**G**	**L**	**R**		**Q**	**R**	**D**	**Q**	**T**	**Q**	**K**	S	**P**	**T**	60					
E	**G**	**P**	F	K	**R**	**E**	E	**L**	M	A		**H**	**L**	**E**	Q	**Q**	**A**	K	D	I	**K**	79					
SK	**G**	**P**	L	D	**R**	**E**	A	**L**	L	Q		**H**	**L**	**E**	K	**Q**	**A**	L	E	A	**K**	80					
									a	*b*		*c*	*d*	*e*	*f*	*g*	*a*	*b*	*c*	*d*	*e*						
E	D	**R**	**E**	**D**	**L**	**V**	**P**	**F**	**T**	**G**		**E**	**K**	R	**G**	**K**	A	W	I	**P**	**K**	99					
Sk	E	**R**	**E**	**D**	**L**	**V**	**P**	**F**	**T**	**G**		**E**	**K**	K	**G**	**K**	P	F	V	**P**	**K**	100					
	f	*g*																									
E	Q	K	P	M	D	P	V	L	**E**	S		V	T	-	**L**	**E**	**P**	**E**	**L**	**E**	**E**	118					
Sk	N	P	T	R	E	I	P	R	**E**	E		Q	I	T	**L**	**E**	**P**	**E**	**L**	**E**	**E**	120					
E	**A**	**L**	A	**N**	**A**	S	D	**A**	**E**	L		C	D	(E	F)												
Sk	**A**	**L**	A	**N**	**A**	T	E	**A**	**E**	M																	

FIGURE 2 Sequences and alignment of Sk-Tmod$_{1–130}$ with E-Tmod$_{1–130}$. The fragments contain residues 1 to 130 of chicken Sk- and E-Tmod (Almenar-Queralt et al., 1999) plus a portion of the glutathione S-transferase linkers. The N-terminal glutathione S-transferase linkers and C-terminal residues not from the sequence of the Tmods are given in parentheses. For comparison of Sk-Tmod with E-Tmod, the residues are numbered using the sequence of the native Tmod, and identical residues are bold faced. The N-terminal linkers are not numbered. Residues with high propensity to form coiled-coils are shaded and the heptad repeats are written below in italics.

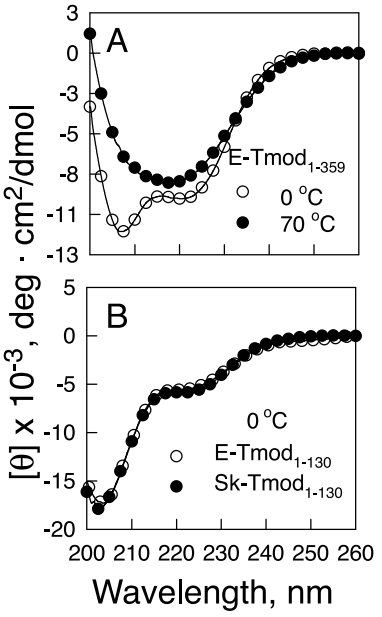

FIGURE 3 (*A*) Mean residue ellipticity of recombinant E-Tmod$_{1–359}$. (○) 0°C; (●) 70°C. (*B*) Mean residue ellipticty of (○) Sk- and (●) E-Tmod$_{1–130}$ at 0°C. The recombinant fragments and proteins were all 10 μM, in 100 mM NaCl, 10 mM sodium phosphate, pH 6.5.

two-chained coiled-coil α-helices as reported previously (Greenfield et al., 1998, 2001).

Binding of the TM chimeras to full length E-Tmod causes changes in structure and stability

Binding of either AcTM1aZip or AcTM1bZip to E-Tmod$_{1–359}$ caused large increases in the thermal stability of the complexes compared with the sum of the unmixed components. The T_Ms of unfolding of AcTM1aZip and AcTM1bZip, 10 μM, were 25 and 44°C, respectively. Addition of equimolar E-Tmod$_{1–359}$ increased the T_Ms to 65 and 61°C, respectively (data not shown). The unfolding of the E-Tmod-TMZip complexes was highly cooperative and complete. However, the changes in ellipticity attributable to complex formation were small, and the unfolding of Tmod$_{1–359}$–TMZip complexes was not reversible. We therefore decided to use shorter Tmod fragments, where the folding of the TMZip-Tmod fragment complexes were reversible, to determine if there was isoform specificity in the binding interactions. We had shown previously that the binding sites for long and short TMs were contained within this N-terminal region of Tmod (Babcock and Fowler, 1994; V.M. Fowler, unpublished data).

Complex formation between the TMZips and the Tmod fragments results in increased α-helix and β-sheet content and stability

The binding of either Tmod$_{1–130}$ isoform to either TMZip caused increases in negative ellipticity with maxima near

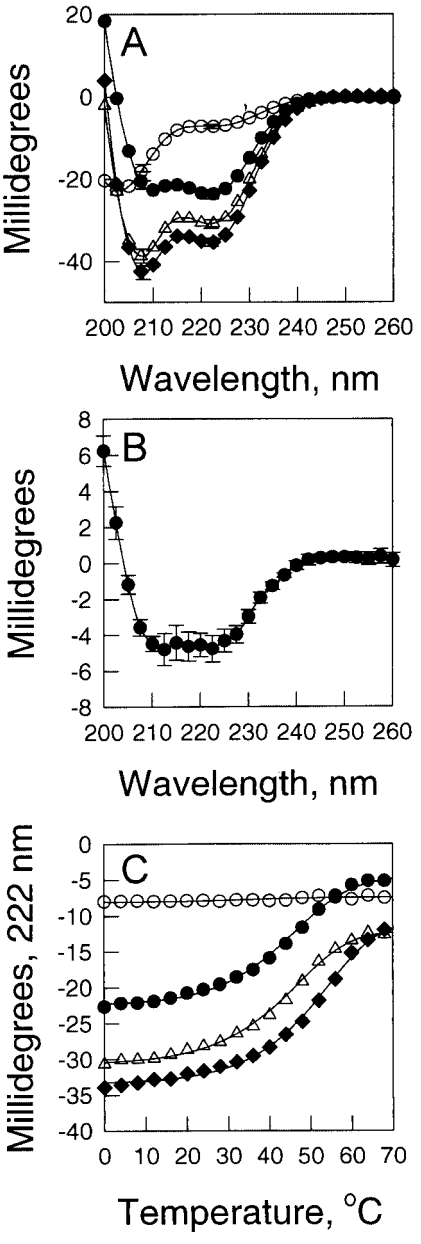

FIGURE 4 (*A*) Circular dichroism spectra of (○) E-Tmod$_{1–130}$, (●) AcTM1bZip, (△) the sum of the spectra of E-Tmod$_{1–130}$ and AcTM1bZip and (◆) the spectrum of the mixture E-Tmod$_{1–130}$ and AcTM1bZip. Data are the average and standard error of four to seven measurements. (*B*) Difference between the spectrum of the mixture of the components and the sum of the unmixed components in A. Data are the average and standard error of four measurements. (*C*) Ellipticity at 222 nm of the unmixed and mixtures of the components in *A* as a function of temperature. Symbols same as *A*. Curves are the average values of three to seven measurements. E-Tmod$_{1–130}$ and AcTM1aZip were both 10 μM, in 100 mM NaCl, 10 mM sodium phosphate, pH 6.5.

222, 218, and 208 nm compared with the unmixed components. The bands at 222 and 208 are characteristic of increases in α-helical content, and the band at 218 nm is characteristic of increases in β-structure. The effect of mix-

TABLE 1 Characterization of the secondary structure induced by AcTMZip-Tmod$_{1–130}$ complex formation*

AcTMZip	Tmod$_{1–130}$	Replicates	α-Helix	β-Sheet	β-Turn
1a	Sk	3	77 ± 5	23 ± 5	0
1b	Sk	3	52 ± 3	47 ± 5	1 ± 1
1a	E	5	58 ± 3	42 ± 4	2 ± 1
1b	E	E	58 ± 8	41 ± 8	1 ± 1

*The circular dichroism difference spectra between the complexes of the TMZips and Tmod fragments and the sum of the individual spectra between 240 and 200 nm were fit by nonconstrained multiple linear regression (Brahms and Brahms, 1980; Greenfield, 1996) using the spectra of polypeptides with known conformaiton as references (Brahms and Brahms, 1980). All components were 10 μM in 100 mM NaC1, 10 μM sodium phosphate, pH 6.5 at 0°C.

ing E-Tmod$_{1–130}$ with AcTM1bZip is illustrated in Fig. 4. The average differences in molar ellipticity at 222 nm upon complex formation among the four combinations of the Tmod$_{1–130}$ fragments and TMZips ranged from -3.6 ± 0.9 to $-5.8 \pm 0.5 \times 10^5$ degrees $\times$ cm^2/dmol (mean ± SD) and were not statistically different from one another. The difference spectra were fit by nonconstrained multilinear regression to estimate what proportion of the structural changes were due to increased α-helix or increased β-structure. Because multilinear regression relies only on the shape of the CD curves to estimate secondary structure it is less accurate than other methods and only gives estimates of α-helical and β-structure content to accuracies of approximately ±16% of the total secondary structure (Greenfield, 1996). Given this caveat, from the shape of the CD difference curves, the secondary structural change induced by binding appears to be approximately 50% to 70% α-helical with the rest β-sheet (Table 1). This combination of secondary structures would be expected to have a mean residue ellipticity near $-20{,}000$ degrees $\times$ cm^2/dmol at 222 nm. The increase in molar ellipticity of the complex was approximately $-500{,}000$ degrees $\times$ cm^2/dmol, suggesting that ~25 residues of the Tmod N-terminal fragments become ordered upon TMZip binding.

Binding of E- or Sk-Tmod$_{1–130}$ to either TMZip also greatly increased the stability of the complexes compared with the unmixed components (e.g., Fig. 4 *C*). In addition, the complexes unfolded in single two-state transitions with higher cooperativity than unfolding of the TMZip two-chained coiled coils. The thermodynamic parameters of unfolding of the individual components and complexes are given in Table 2.

Effect of N-terminal modifications of TM and TMZips on Tmod affinity

In vivo, TMs are acetylated at the N terminus during post-translational processing and the acetyl group is an important determinant of function in striated muscle TM. Unacetylated striated TM has greatly reduced affinity for actin, compared with native acetylated TM, and polymerizes poorly by the criteria of high shear viscosity (Cho et al., 1990; Urbancikova and Hitchcock-DeGregori, 1994).

Binding of Sk- and E-Tmods to native and recombinant TMs, which lack N-terminal acetyl groups, were probed using blot overlays (Fig. 5). Both Sk- and E-Tmods bound to N-acetylated chicken skeletal muscle striated α-TM. However, the affinities of both Tmods for unacetylated recombinant striated muscle TM or TM2 (which differs at the C terminus) were greatly reduced, as binding was not detected in the blot overlays. In contrast, both E- and Sk-Tmods bound strongly to unacetylated short TMs, with the N termini encoded by exon 1b. Interestingly, Sk-Tmod bound to native striated muscle TM and to the unacetylated short TMs with similar affinity (Fig. 5 *A*) whereas E-Tmod bound better to the short TMs than to the native striated muscle α-TM (Fig. 5 *B*) (also see below).

We tested the effect of N-terminal modifications on the thermodynamics of folding of the TMZips and their ability to interact with E- and Sk-Tmod$_{1–130}$ (Tables 2 and 3, Fig. 6). Modifications to TM1aZip that destroy its ability to form a coiled coil also resulted in loss of Tmod binding ability. Fig. 6 shows that GlyTM1aZip (Fig. 6 *B*) was less stable than AcTM1aZip (Fig. 6 *A*), but it formed a fully folded coiled-coil at low temperatures and it bound to Sk-Tmod$_{1–130}$ with the same affinity as the acetylated TM1aZip (Table 3). Removal of the acetyl group entirely, however, significantly decreased the helical content of the fully folded TM1aZip and the unacetylated form did not bind to either the Sk- (Fig. 6 *C*) or E-Tmod$_{1–130}$ fragment (not shown) at a concentration of 10 μM.

Replacement of the N-terminal acetyl in TM1bZip with Gly had very little effect on its stability and its binding affinity for the Tmod fragments (Tables 2 and 3). This result was not surprising because nuclear magnetic resonance spectra of AcTM1bZip and GlyTM1bZip are virtually superimposable, showing that they have the same structure (Greenfield et al., 2001).

Effect of a nemaline myopathy mutation (Met-8-Arg) on the binding of AcTM1aZip to Sk- and E-Tmod$_{1–130}$

Mutations in a human skeletal muscle TM encoded by the *TPM3* gene cause nemaline myopathy, a rare congenital skeletal muscle disease with associated muscle weakness, reviewed by Laing (1999). Nemaline rods, which are composed of actin filaments and α-actinin, are found at the *Z* line in muscle and are a characteristic of the disease, implying that the mutations may affect thin filament assembly or stability (Yamaguchi et al., 1982). In one mutation, a methionine at the coiled-coil interface of TM, (Met-8), is mutated to arginine (Laing et al., 1995; Laing, 1999). The Met-8-Arg mutation reduces the affinity of recombinant striated α-TM for actin more than 100-fold and also impairs

TABLE 2 Thermodynamics of unfolding of TMZip-Tmod$_{1-130}$ complexes*

TMZip N-terminal modification	Parameter	TM1aZip alone	Tm1aZip-E-Tmod complex	TM1aZip-Sk-Tmod complex	TM1bZip alone	TM1bZip-E-Tmod complex	TM1bZip-Sk-Tmod complex
Acetyl	ΔH	32. ± 0.5	43.3 ± 1.8	44.7 ± 0.8	35.4 ± 0.2	55.4 ± 8.6	48.1 ± 2.0
	T_M°X	25.1 ± 0.1	33.8 ± 0.3	33.4 ± 0.4	44.5 ± 0.9	51.6 ± 1.1	49.5 ± 1.5
	$(\theta]_F$	−34.3 ± 1.6	−17.2 ± 3.8	−16.5 ± 1.2	−30.8 ± 2.7	−14.9 ± 2.2	−16.9 ± 1.3
	$[\theta]_U$	−7.7 ± 0.7	−6.3 ± 1.3	−6.2 ± 0.3	−5.1 ± 0.8	−5.8 ± 0.6	−5.3 ± 0.5
Glycine	ΔH	27.1		−40.0	32.7 ± 4.8	50.0 ± 3.4	47.1
	T_M,°C	15.4		30.8	43.1 ± 1.2	55.1 ± 1.2	56.7
	$[\theta]_F$	−39.1		−15.3	−33.2 ± 2.8	−14.5 ± 0.5	−15.2
	$[\theta]_U$	−6.8		− 5.5	−6.3 ± 1.5	−4.3 ± 0.5	−4.5
None	ΔH	29.2 ± 4.6					
	T_M,°C	13.8 ± 1.0					
	$[\theta]_F$	−15.9 ± 7.6					
	$[\theta]_U$	−6.1 ± 0.0					

*The apparent enthalpy and T_M of unfolding were estimated from the change of ellipticity at 222 nm as a function of temperature assuming that ΔCp of unfolding was zero. TMZips were 10 μM, and the TMZip-Tmod complexes were the 1:1 mixtures of 10 μM TMZip (two-chains) + 10 μM E- or SK-Tmod$_{1-130}$ in 100 mM NaC1, 10 mM sodium phosphate pH 6.5. The enthalpy values are reported in Kcal/mol, and the reported T_M values are the values at 10 μM determined from the curve fits. $[\theta]_F$ is the mean residue ellipticity in degree × cm^2/dmol of the fully folded and $[\theta]_U$ is the mean residue ellipticity of the fully unfolded TMZip or TM-Tmod complex. Data reported with reported standard deviations were from two to five replicate experiments. Otherwise they are the results from single measurement.

regulatory function (Moraczewska et al., 2000). The mutation also greatly reduces the helical content and stability of AcTM1aZip (Moraczewska et al., 2000). There were no circular dichroism changes when Tmod was added to AcTM1aZip when Met-8 was replaced with Arg (Table 3), suggesting that the mutation destroys the ability of AcTM1aZip to interact with Tmod. An inability of TM to interact with Tmod may affect the assembly or stability of thin filaments in diseased muscle.

Binding specificities of the Tmod$_{1-130}$ fragments for the TMZips

The stoichiometry of binding of AcTM1bZip and AcTM1aZip for Sk- and E-Tmod$_{1-130}$ were determined at 30°C by titrating the TMZips with the Tmod fragments and following the formation of the complexes by the increases in ellipticity at 222 nm. This temperature was chosen because it showed the greatest difference in ellipticity between the bound and unbound AcTM1aZIp complexes. Fig. 7 shows representative titration curves. In all cases the ellipticity change saturated at a 1:1 molar equivalent of Tmod$_{1-130}$ (one chain) to TMZip (two chains). There was a greater ellipticity increase when the Tmods$_{1-130}$ bound to AcTM1aZip than AcTM1bZip, because AcTM1aZip is approximately 50% unfolded whereas AcTM1bZip is less than 10% unfolded at 30°C.

The thermodynamic parameters, summarized in Table 2, were used to determine the binding constants of the Tmod$_{1-130}$-TMZip complexes assuming that all of the changes in free energy between the two-chained TMZips and the three-chained TMZip-Tmod binary complexes were due to complex formation and that $K_d = 1/e^{-\Delta\Delta G/nRT}$. The thermodynamic data showed that the affinity of the E-Tmod fragment was four- to fivefold higher for AcTM1bZip than AcTM1aZip (K_d = 0.23 ± 0.15 μM, N = 3 versus 1.1 ± 0.4 μM, N = 4, $p < 0.01$), but that the Sk-Tmod fragment had approximately equal affinity for both TMZips (K_d = 0.6 ± 0.1 μM, N = 2 versus 0.7 ± 0.3 μM, N = 3, not significantly different). This is similar to the qualitative differences in Sk and E-Tmod binding to short and long TMs observed in blot overlays (Fig. 5).

The binding constants were also estimated from the binding isotherms shown in Fig. 7. At the concentration used in the titrations, 10 μM, the binding was too tight to give highly accurate binding constants, but the two methods agreed with each other.

Table 3 summarizes the dissociation constants, the increases in ellipticity at 222 nm at 0°C upon complex formation, $\Delta\theta$, and the changes in the midpoint of the major unfolding transition upon complex formation, ΔT_M of all of the TMZip-Tmod$_{1-130}$ complexes.

DISCUSSION

N-terminal coiled coil of TM must be intact for Tmod to bind

Our results show that the ability of the N terminus of tropomyosin to form a complete coiled coil (starting at residue 1 in the TM1aZips, and at residue 6 in the TM1bZips) when fully folded is essential for its interaction with tropomodulin, although binding can still occur when the TMZip peptides are in a equilibrium with the unfolded peptides at high temperatures. For example, at 30°C, the TM1aZip peptide is in a dynamic two-state equilibrium

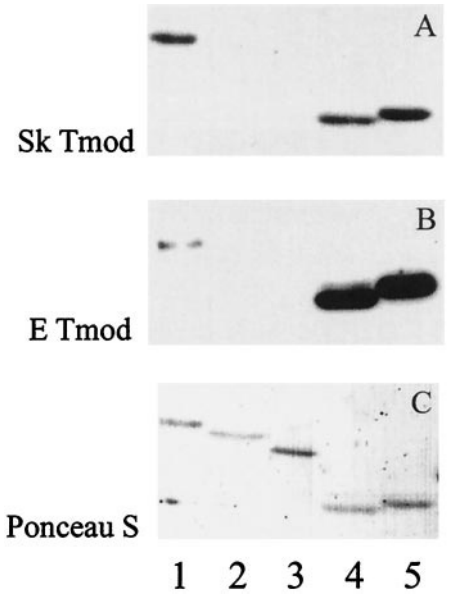

FIGURE 5 Sk- and E-Tmods bind to acetylated long striated TM and unacetylated short TMs but not to unacetylated striated or smooth long TMs on blot overlays. Each 0.1 μg of TM was electrophoresed on a 12% sodium dodecyl sulfate-polyacrylamide mini-gel (Laemmli, 1970) and transferred to nitrocellulose (Towbin et al., 1979). After blocking with 4% bovine serum albumin and incubation with 1 μg/mL purified recombinant chicken Sk-Tmod or E-Tmod, binding of the Tmods to the TMs was detected by incubation with affinity-purified rabbit anti-E- or Sk-Tmod antibodies (McElhinny et al., 2001) followed by standard chemiluminescence procedures. The TM proteins were detected by staining with Ponceau S. (*A*) Sk-Tmod binding probed with rabbit antibody 3577; (*B*) E-Tmod binding probed with rabbit antibody 1844; (*C*) Tropomyosins visualized with Ponceau S. (Lane 1) Native chicken striated TM; (Lane 2) Recombinant rabbit striated muscle TM (TM1a9a); (Lane 3) Recombinant rabbit TM2 (TM1a9d); (Lane 4) unacetylated nonmuscle TM5a (TM 1b9d); (Lane 5) recombinant chimeric TM (TM1b9a). The recombinant proteins are not acetylated. Note that the relative binding of E-Tmod to a particular TM cannot be compared directly with the binding of Sk-Tmod to that TM because the antibodies used for E and Sk-Tmod detection were different.

TABLE 3 Binding of tropomodulin peptides to tropomyosin peptides

TMZip	$Tmod_{1-130}$	N-Terminal modification	ΔT_M*	$\Delta\theta$, 222 nm millidegrees†	K_d, 30°C μM‡
1a	E	Ac	10.8 ± 2.2	−3.6 ± 0.9	1.1 ± 0.4
1a	E	None	0	0	
1b	E	Ac	8.7 ± 2.2	−5.3 ± 1.5	0.2 ± 0.2
1b	E	Gly	12.2 ± 0.0	−3.0 ± 0.6	0.4 ± 0.1
1a	Sk	Ac	11.0 ± 2.3	−5.8 ± 0.5	0.7 ± 0.3
1a	Sk	Gly	16.9	−5.8	0.5
1a	Sk	None	0		
1b	Sk	Ac	5.7 ± 2.4	−5.3 ± 0.6	0.6 ± 0.1
1b	Sk	Gly	10.0	−1.5	0.7
M8R1a	E	Ac	0	0	
M8R1a	SK	Ac	0	0	

*The difference in the observed midpoints of the cooperative unfolding transitions (determined from the first derivative of the unfolding curves) of the mixture of the TMZip and Tmod fragments and the additions of the curves for the TMZip and Tmod fragments alone.
†The increase in ellipticity at 222 nm at 0°C of the mixed Tmod fragments and TMZips compared with the sum of the individual spectra.
‡The K_d values were estimated from the thermodynamics of unfolding of the $Tmod_{1-130}$-TMZip complexes compared with the Tmod fragments and TMZips alone. All components were 10 μM in 100 mM NaC1, 10 mM sodium phosphate, pH 6.5. Data with standard deviations are the mean of two to five replicate measurements. Otherwise they are the results of a single experiment.

between the folded and unfolded forms. Addition of the tropomodulin fragments shifts the equilibrium to the folded form. Modifications that prevent the complete folding of the coiled-coil structure of the N terminus, however, such as removal of the N-terminal acetyl group from the long TMs or introduction of a disease producing mutation at the coiled-coil interface result in loss of binding affinity for Tmod.

Comparison of atomic resolution structures of AcTm1aZip with an unacetylated 81-residue fragment of chicken striated α-TM, Tm81, (Brown et al., 2001), which shares the same N terminus, gives insight into the effect of N-acetylation on the structure of the N terminus of long TMs. In acetylated AcTM1aZip (Fig. 8 *A*), the side-chains of Met-1 (see arrows) are part of the coiled coil and interact with one another across the helix-helix interface and with the side-chains of Ile-4 of the opposite chain (Greenfield et al., 1998). In unacetylated Tm81 (Fig. 8 *B*), however, the side-chains of Met-1 (see arrows) from the two chains are not part of the coiled-coil, which now begins at Ala-3, and the Met-1 residues are in close proximity to the side-chains of Gln-9 and Lys-6 from the same chain.

Unacetylated recombinant striated muscle TM also binds poorly to actin, but the weak affinity is greatly increased when the protein is expressed with a variety of N-terminal fusion peptides as short as two amino acid residues (Hitchcock-DeGregori and Heald, 1987; Heald and Hitchcock-DeGregori, 1988; Monteiro et al., 1994; Urbancikova and Hitchcock-DeGregori, 1994). We found that replacing the N-terminal acetyl group with Gly alone, allows the TM1aZip to form a fully folded α-helical coiled coil and is sufficient to restore the ability of TM1aZip to bind to Tmod.

The Met-8-Arg nemaline myopathy mutation also destroys the N-terminal coiled coil of TM and prevents its binding to Tmod, again showing the necessity of an intact N-terminal coiled coil. Removal of the N-terminal acetyl group from the 1b TMs has no negative effects on its ability to bind to Tmod, probably because the first five residues, with the sequence AGSSS, are sufficient to stabilize the N-terminal coiled-coil of TM1bZip that starts at residue 6.

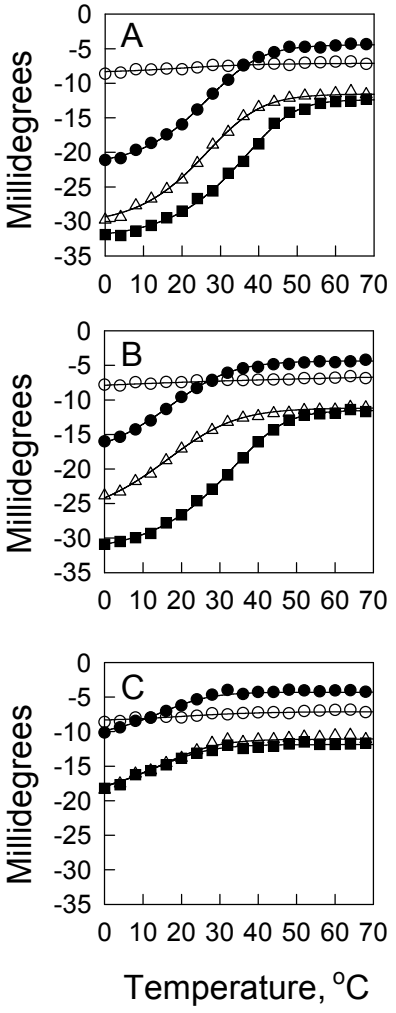

FIGURE 6 Circular dichroism at 222 nm of Sk-Tmod$_{1–130}$, with AcTM1aZip (*A*), GlyTM1aZip (*B*) and unacetylated TM1aZip (*C*) and their mixtures as a function of temperature. (○) SkTmod$_{1–130}$; (●) TM1aZip; (△) addition of curves of TM1aZip and SkTmod$_{1–130}$; (■) mixture of TM1aZip and Tmod$_{1–130}$. Conditions same as Fig. 4.

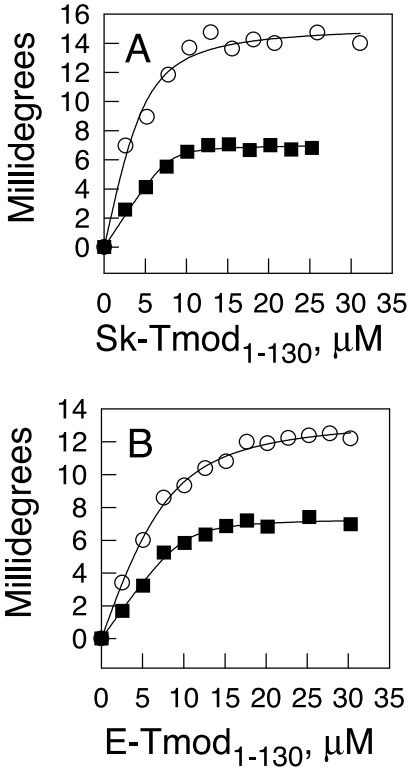

FIGURE 7 Increase in ellipticity at 222 nm, 30°C, when Sk-Tmod$_{1–130}$ (*A*) and E-Tmod$_{1–130}$ (*B*) bind to AcTM1aZip (○) and AcTM1bZip (■). 0.5 mL of the TMZips, 10 μM, in 100 mM NaCl, 10 mM sodium phosphate, pH 6.5 in 2-mm pathlength cells, were titrated with concentrated solutions of the Tmod constructs. The ellipticity changes were corrected for the ellipticity of the Tmod fragments alone and for dilution (from 0.5 to 0.7 mL).

Nature of the structural changes when TM binds to Tmod is consistent with formation of a coiled coil

Binding of Tmod$_{1–130}$ to the TMZips stabilizes the structure and induces α-helical and β-sheet structure in Tmod. Coiled coil are characterized by sequences with heptad repeats, usually labeled *a*, *b*, *c*, *d*, *e*, *f*, and *g*. In coiled coils, residues at *a* and *d* positions are usually hydrophobic or alanine, whereas residues at *b*, *c*, *e*, *f*, and *g* positions are hydrophilic (Cohen and Parry, 1990, 1994; Lupas et al., 1991; Lupas, 1997). By inspection, E- and Sk-Tmod both have two short regions in their N-terminal domains with repeating heptad sequences (see highlighted residues in Fig. 2): residues 24 to 38 and 68 to 81 in E-Tmod and residues 25 to 39 and 69 to 82 in Sk-Tmod. A possible model of the Tmod$_{1–130}$ and TMZip complex is that the N-terminal coiled coil of TMZip could interact with the heptad repeat sequences of Tmod$_{1–130}$ to form a three- or four-stranded coiled-coil interface. Examination of helical wheel models of the Tmod heptad repeat regions docked to TM1aZip and TM1bZip shows that both Tmod heptad repeat regions have the propensity to form three-stranded coiled coils with TMZip as judged by the presence of favorable packing interactions with the residues in the *a* and *d* positions, and favorable charge-charge interactions of residues at the *e* and *g* positions. The interaction may also induce the formation of β-structure in the TM binding domain of Tmod, which may contribute to the ability of Tmod-TM to cap the pointed end of the actin filament.

Specificity of the interaction of the short and long TM isoforms to E-Tmod is determined by the TM N terminus

Using CD spectroscopy we found that E-Tmod$_{1–130}$ had approximately fourfold higher affinity for AcTM1bZip than AcTM1aZip and that both AcTMZips had equal affinity to Sk-Tmod$_{1–130}$. Thus, the N-terminal sequence of the TMs

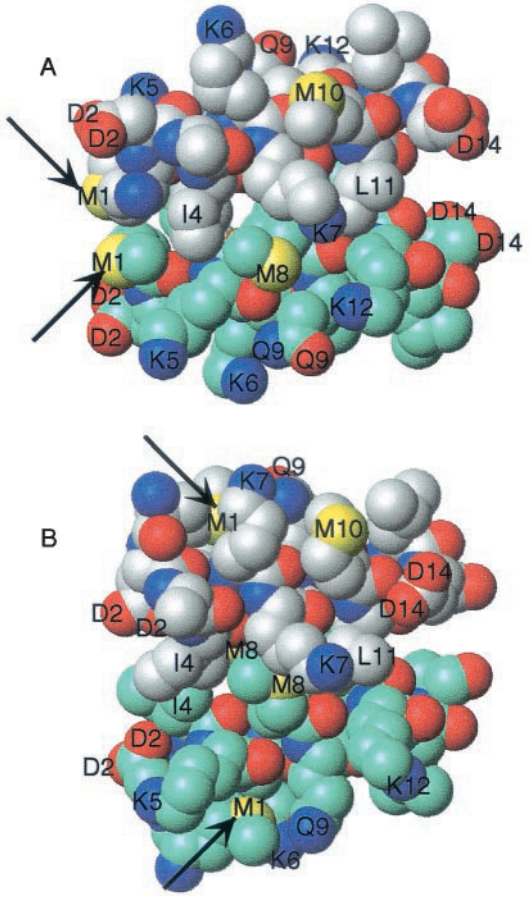

FIGURE 8 Effect of N-acetylation on the structure of the N terminus of long TMs (residues 1–14). (*A*) Acetylated TM, solution structure of AcTM1aZip determined from two-dimensional nuclear magnetic resonance (coordinates from PDB file 1tmz). (*B*) Unacetylated TM: crystal structure of unacetylated TM80 determined by x-ray crystallography (coordinates from PDB file 1IC2). Arrows point to the N-terminal Met-1 residues. In the acetylated peptide the first two residues are part of the coiled coil, but they are not helical in the unacetylated peptide. In the models, the side-chains of the hydrophobic residues at *a* and *d* positions of the coiled-coil heptad repeat and the noncarbon atoms of the hydrophilic side-chains are labeled with the residue number. The carbon atoms of chain 1 are in gray and of chain two are in aqua. Nitrogen atoms are blue, oxygen atoms are red, and sulfur atoms are yellow. The molecular models were prepared using MolMol. (Koradi et al., 1996).

determines the specificity for E-Tmod. These difference in TM isoform recognition may be determined by residues 100 to 111 of E-Tmod$_{1-130}$, which are the regions least conserved with Sk-Tmod (Fig. 2). Our results are in agreement with some previous studies, suggesting that the interactions of TMs with the Tmods are isoform specific (Sussman and Fowler, 1992; Watakabe et al., 1996). Both Sussman and Fowler (1992) and Watakabe et al. (1996) observed that E-Tmod bound better to erythrocyte (a short TM) and other short TMs than to skeletal muscle (a long) TM. We also observed that E-Tmod bound preferentially to recombinant TM5a, a short nonmuscle α-TM, as compared with native striated muscle α-TM (a long TM). On the other hand, a previous study (Babcock and Fowler, 1994) suggested that E-Tmod had approximately equal affinity for erythrocyte and skeletal muscle TMs. The reason for these discrepant results are not clear but may be due to the use of the harsh Bolton-Hunter reagent to iodinate the TMs for the binding assays by Babcock et al. (1994).

The structures of the backbones of the coiled-coil regions of AcTM1aZip and AcTM1bZip coiled-coil regions are almost identical, but there are differences in the N termini and structural dynamics of the two chimeric proteins. AcTM1aZip is a coiled coil to its extreme N terminus and unfolds in a single cooperative transition (Greenfield et al., 1998). nuclear magnetic resonance studies of GlyTM1bZip (Greenfield et al., 2001) showed that residues 1 to 6 are not helical and residues 7 to 9, the first three residues of the coiled-coil domain, unfold before the rest of the molecule. Moreover, the side-chain of Ile-14 in AcTM1bZip has multiple conformations, even at temperatures where the molecule is fully folded. Conformational flexibility is often important to allow optimal packing interactions. Indeed it has been found that mutation of Val-10 and Ile-14 to Leu in hTM5, a short TM, which would change the packing interactions, and make a coiled-coil peptide more stable, destroyed its ability to interact with Tmod (Vera et al., 2000). The differences in the topology and flexibility between the coiled-coil interfaces of the 1a and 1b encoded N termini of the tropomyosins could affect their binding interactions with the Tmods and be responsible for the specificity of binding to E-Tmod.

SUMMARY

Studies using TM and Tmod model proteins have given insight into the mechanism and structural requirements of the interactions of tropomyosin with tropomodulin. Tmod and TM form 1:1 complexes, one chain of Tmod/two chains of TM. TM binding causes conformational changes in Tmod including increased α-helix and β-structure. The increase in helical content along with examination of the sequences of the Tmods suggests that the interface between TM and Tmod may include a three or four-stranded coiled-coil. N-terminal acetylation, which stabilizes the coiled-coil of the N terminus of long TMs, is crucial for interaction of the long TMs with Tmod. A mutation that causes nemaline myopathy in a long TM (Met-8-Arg) severely impairs their ability to interact with either Sk- or E-Tmod, suggesting the mutation could severely affect actin filament length and sarcomere assembly.

We would like to thank Jeannette Moyer for purification of the recombinant tropomodulin fragments and Kim Fritz-Six for construction of the expression constructs and performing the blot-overlay experiments. We would also like to thank Yuhua Sung and Joanna Moraczewska for preparation of the recombinant and muscle tropomyosins used in the blot-

overlay experiments and Thomas Palm who supplied GlyTM1bZip. Finally, we owe great thanks to Sarah Hitchcock-DeGregori for her critical reading of the manuscript and many helpful suggestions. This work was funded by National Institutes of Health grants HL-35726 and GM-36326 (to S.E.H.D. and N.J.G.) and GM-34225 (to V.M.F.).

REFERENCES

Almenar-Queralt, A., A. Lee, C. A. Conley, L. Ribas de Pouplana, and V. M. Fowler. 1999. Identification of a novel tropomodulin isoform, skeletal tropomodulin, that caps actin filament pointed ends in fast skeletal muscle [published erratum appears in *J. Biol. Chem.* 2000. 275:13164]. *J. Biol. Chem.* 274:28466–28475.

Babcock, G. G., and V. M. Fowler. 1994. Isoform-specific interaction of tropomodulin with skeletal muscle and erythrocyte tropomyosins. *J. Biol. Chem.* 269:27510–27518.

Bailly, M., F. Macaluso, M. Cammer, A. Chan, J. E. Segall, and J. S. Condeelis. 1999. Relationship between Arp2/3 complex and the barbed ends of actin filaments at the leading edge of carcinoma cells after epidermal growth factor stimulation. *J. Cell. Biol.* 145:331–345.

Bamburg, J. R., A. McGough, and S. Ono. 1999. Putting a new twist on actin: ADF/cofilins modulate actin dynamics. *Trends Cell Biol.* 9:364–370.

Blanchoin, L., T. D. Pollard, and S. E. Hitchcock-DeGregori. 2001. Inhibition of the Arp2/3 complex-nucleated actin polymerization and branch formation by tropomyosin. *Curr. Biol.* 11:1300–1304.

Bohm, G., R. Muhr, and R. Jaenicke. 1992. Quantitative analysis of protein far UV circular dichroism spectra by neural networks. *Protein Eng.* 5:191–195.

Brahms, S., and J. Brahms. 1980. Determination of protein secondary structure in solution by vacuum ultraviolet circular dichroism. *J. Mol. Biol.* 138:149–178.

Broschat, K. O. 1990. Tropomyosin prevents depolymerization of actin filaments from the pointed end. *J. Biol. Chem.* 265:21323–21329.

Broschat, K. O., A. Weber, and D. R. Burgess. 1989. Tropomyosin stabilizes the pointed end of actin filaments by slowing depolymerization. *Biochemistry.* 28:8501–8506.

Brown, J. H., K. H. Kim, G. Jun, N. J. Greenfield, R. Dominguez, N. Volkmann, S. E. Hitchcock-DeGregori, and C. Cohen. 2001. Deciphering the design of the tropomyosin molecule. *Proc. Natl. Acad. Sci. U. S. A.* 98:8496–8501.

Cho, Y. J., J. Liu, and S. E. Hitchcock-DeGregori. 1990. The amino terminus of muscle tropomyosin is a major determinant for function. *J. Biol. Chem.* 265:538–545.

Cohen, C., and D. A. Parry. 1990. Alpha-helical coiled coils and bundles: how to design an alpha-helical protein. *Proteins.* 7:1–15.

Cohen, C., and D. A. Parry. 1994. Alpha-helical coiled coils: more facts and better predictions. *Science.* 263:488–489.

Conley, C. A., K. L. Fritz-Six, A. Almenar-Queralt, and V. M. Fowler. 2001. Leiomodins: larger members of the tropomodulin (tmod) gene family. *Genomics.* 73:127–139.

Cox, P. R., and H. Y. Zoghbi. 2000. Sequencing, expression analysis, and mapping of three unique human tropomodulin genes and their mouse orthologs. *Genomics.* 63:97–107.

Edelhoch, H. 1967. Spectroscopic determination of tryptophan and tyrosine in proteins. *Biochemistry.* 6:1948–1954.

Engel, G. 1974. Estimation of binding parameters of enzyme-ligand complex from fluorometric data by a curve fitting procedure: seryl-tRNA synthetase-tRNA Ser omplex. *Anal. Biochem.* 61:184–191.

Engel, J., H. T. Chen, D. J. Prockop, and H. Klump. 1977. The triple helix in equilibrium with coil conversion of collagen-like polytripeptides in aqueous and nonaqueous solvents: comparison of the thermodynamic parameters and the binding of water to (L-Pro-L-Pro-Gly)n and (L-Pro-L-Hyp-Gly)n. *Biopolymers.* 16:601–622.

Fanning, A. S., J. S. Wolenski, M. S. Mooseker, and J. G. Izant. 1994. Differential regulation of skeletal muscle myosin-II and brush border myosin-I enzymology and mechanochemistry by bacterially produced tropomyosin isoforms. *Cell Motil. Cytoskeleton.* 29:29–45.

Fasman, G. D. 1989. Practical Handbook of Biochemistry and Molecular Biology. CRC Press, Baton Raton, FL.

Fowler, V. M. 1987. Identification and purification of a novel Mr 43,000 tropomyosin-binding protein from human erythrocyte membranes. *J. Biol. Chem.* 262:12792–12800.

Fowler, V. M. 1990. Tropomodulin: a cytoskeletal protein that binds to the end of erythrocyte tropomyosin and inhibits tropomyosin binding to actin. *J. Cell Biol.* 111:471–481.

Fowler, V. M., and C. A. Conley. 1999. Tropomodulin. *In* Guidebook to the Cytoskeletal and Motor Proteins, 2nd ed. T.E. Kreis and R.D. Vale, editors. Oxford University Press, Oxford, United Kingdom. 154–159.

Greenfield, N. J. 1996. Methods to estimate the conformation of proteins and polypeptides from circular dichroism data. *Anal. Biochem.* 235: 1–10.

Greenfield, N. J., and S. E. Hitchcock-DeGregori. 1993. Conformational intermediates in the folding of a coiled-coil model peptide of the N-terminus of tropomyosin and alpha alpha-tropomyosin. *Protein Sci.* 2:1263–1273.

Greenfield, N. J., and S. E. Hitchcock-DeGregori. 1995. The stability of tropomyosin, a two stranded coiled-coil protein, is primarily a function of the hydrophobicity of residues at the helix-helix interface. *Biochemistry.* 34:16797–16805.

Greenfield, N. J., J. H. Huang, T. Palm, G. V. T. Swapna, D. Monleon, G. T. Montelione, and S. E. Hitchcock-DeGregori. 2001. Solution NMR structure and folding dynamics of the N terminus of a rat non-muscle α-tropomyosin in an engineered chimeric protein. *J. Mol. Biol.* 312: 833–847.

Greenfield, N. J., G. T. Montelione, R. S. Farid, and S. E. Hitchcock-DeGregori. 1998. The structure of the N-terminus of striated muscle alpha-tropomyosin in a chimeric peptide: nuclear magnetic resonance structure and circular dichroism studies. *Biochemistry.* 37:7834–7843.

Gregorio, C. C., and V. M. Fowler. 1995. Mechanisms of thin filament assembly in embryonic chick cardiac myocytes: tropomodulin requires tropomyosin for assembly. *J. Cell Biol.* 129:683–695.

Gregorio, C. C., A. Weber, M. Bondad, C. R. Pennise, and V. M. Fowler. 1995. Requirement of pointed-end capping by tropomodulin to maintain actin filament length in embryonic chick cardiac myocytes. *Nature.* 377:83–86.

Heald, R. W., and S. E. Hitchcock-DeGregori. 1988. The structure of the amino terminus of tropomyosin is critical for binding to actin in the absence and presence of troponin. *J. Biol. Chem.* 263:5254–5259.

Helfman, D. M., S. Cheley, E. Kuismanen, L. A. Finn, and Y. Yamawaki-Kataoka. 1986. Nonmuscle and muscle tropomyosin isoforms are expressed from a single gene by alternative RNA splicing and polyadenylation. *Mol. Cell Biol.* 6:3582–3595.

Hitchcock-DeGregori, S. E., and R. W. Heald. 1987. Altered actin and troponin binding of amino-terminal variants of chicken striated muscle alpha-tropomyosin expressed in *Escherichia coli*. *J. Biol. Chem.* 262: 9730–9735.

Koradi, R., M. Billeter, and K. Wüthrich. 1996. MOLMOL: a program for display and analysis of macromolecular structures. *Mol. Graph.* 14: 51–55.

Kostyukova, A., K. Maeda, E. Yamauchi, I. Krieger, and Y. Maeda. 2000. Domain structure of tropomodulin: distinct properties of the N-terminal and C-terminal halves. *Eur. J. Biochem.* 267:6470–6475.

Laemmli, U. K. 1970. Cleavage of structural proteins during the assembly of the head of bacteriophage T4. *Nature.* 227:680–685.

Laing, N. G. 1999. Inherited disorders of sarcomeric proteins. *Curr. Opin. Neurol.* 12:513–518.

Laing, N. G., S. D. Wilton, P. A. Akkari, S. Dorosz, K. Boundy, C. Kneebone, P. Blumbergs, W. H. S. White, D. R. Love, and E. Haan. 1995. A mutation in the tropomyosin gene TPM3 associated with autosomal dominant nemaline myopathy. *Nat. Genet.* 9:75–79.

Landschulz, W. H., P. F. Johnson, and S. L. McKnight. 1988. The leucine zipper: a hypothetical structure common to a new class of DNA binding proteins. *Science.* 240:1759–1764.

Lin, J. J., T. E. Hegmann, and J. L. Lin. 1988. Differential localization of tropomyosin isoforms in cultured nonmuscle cells. *J. Cell Biol.* 107: 563–572.

Lin, J. J., K. S. Warren, D. D. Wamboldt, T. Wang, and J. L. Lin. 1997. Tropomyosin isoforms in nonmuscle cells. *Int. Rev. Cytol.* 170:1–38.

Littlefield, R., A. Almenar-Queralt, and V. M. Fowler. 2001. Actin dynamics at pointed ends regulates thin filament length in striated muscle. *Nat. Cell Biol.* 3:544–551.

Lupas, A. 1997. Predicting coiled-coil regions in proteins. *Curr. Opin. Struct. Biol.* 7:388–393.

Lupas, A., M. Van Dyke, and J. Stock. 1991. Predicting coiled coils from protein sequences. *Science.* 252:1162–1164.

Marky, L. A., and K. J. Breslauer. 1987. Calculating thermodynamic data for transitions of any molecularity from equilibrium melting curves. *Biopolymers.* 26:1601–1620.

Marquardt, D. W. 1963. An algoritm for the estimation of non-linear parameters. *J. Soc. Indust. Appl. Math.* 11:431–441.

McElhinny, A. S., B. Kolmerer, V. M. Fowler, S. Labeit, and C. C. Gregorio. 2001. The N-terminal end of nebulin interacts with tropomodulin at the pointed ends of the thin filaments. *J. Biol. Chem.* 276:583–592.

Monteiro, P. B., R. C. Lataro, J. A. Ferro, and F. C. Reinach. 1994. Functional α-tropomyosin produced in *Escherichia coli*: a dipeptide extension can substitute the amino-terminal acetyl group. *J. Biol. Chem.* 269:10461–10466.

Moraczewska, J., N. J. Greenfield, Y. Liu, and S. E. Hitchcock-DeGregori. 2000. Alteration of tropomyosin function and folding by a nemaline myopathy-causing mutation. *Biophys. J.* 79:3217–3225.

Moraczewska, J., K. Nicholson-Flynn, and S. E. Hitchcock-DeGregori. 1999. The ends of tropomyosin are major determinants of actin affinity and myosin subfragment 1-induced binding to F-actin in the open state. *Biochemistry.* 38:15885–15892.

Novy, R. E., L. F. Liu, C. S. Lin, D. M. Helfman, and J. J. Lin. 1993. Expression of smooth muscle and nonmuscle tropomyosins in *Escherichia coli* and characterization of bacterially produced tropomyosins. *Biochim. Biophys. Acta.* 1162:255–265.

Palm, T., S. Graboski, S. E. Hitchcock-DeGregori, and N. J. Greenfield. 2001. Disease-causing mutations in cardiac troponin t: identification of a critical tropomyosin-binding region. *Biophys. J.* 81:2827–2837.

Perczel, A., K. Park, and G. D. Fasman. 1992. Analysis of the circular dichroism spectrum of proteins using the convex constraint algorithm: a practical guide. *Anal. Biochem.* 203:83–93.

Small, J. V. 1995. Structure-function relationships in smooth muscle: the missing links. *Bioessays.* 17:785–792.

Sreerama, N., and R. W. Woody. 1994. Poly(pro)II helices in globular proteins: identification and circular dichroic analysis. *Biochemistry* 33: 10022–10025.

Stone, D., and L. B. Smillie. 1978. The amino acid sequence of rabbit skeletal alpha-tropomyosin: the NH2- terminal half and complete sequence. *J. Biol. Chem.* 253:1137–1148.

Sung, L. A., and J. J. Lin. 1994. Erythrocyte tropomodulin binds to the N-terminus of hTM5, a tropomyosin isoform encoded by the gamma-tropomyosin gene. *Biochem. Biophys. Res. Commun.* 201:627–634.

Sussman, M. A., S. Baque, C. S. Uhm, M. P. Daniels, R. L. Price, D. Simpson, L. Terracio, and L. Kedes. 1998. Altered expression of tropomodulin in cardiomyocytes disrupts the sarcomeric structure of myofibrils. *Circ. Res.* 82:94–105.

Sussman, M. A., and V. M. Fowler. 1992. Tropomodulin binding to tropomyosins: isoform-specific differences in affinity and stoichiometry. *Eur. J. Biochem.* 205:355–362.

Svitkina, T. M., and G. G. Borisy. 1999. Progress in protrusion: the tell-tale scar. *Trends Biochem. Sci.* 24:432–436.

Tobacman, L. S. 1996. Thin filament-mediated regulation of cardiac contraction. *Annu. Rev. Physiol.* 58:447–481.

Towbin, H., T. Staehelin, and J. Gordon. 1979. Electrophoretic transfer of proteins from polyacrylamide gels to nitrocellulose sheets: procedure and some applications. *Proc. Natl. Acad. Sci. U. S. A.* 76:4350–4354.

Urbancikova, M., and S. E. Hitchcock-DeGregori. 1994. Requirement of amino-terminal modification for striated muscle alpha-tropomyosin function. *J. Biol. Chem.* 269:24310–24315.

Vera, C., A. Sood, K. M. Gao, L. J. Yee, J. J. Lin, and L. A. Sung. 2000. Tropomodulin-binding site mapped to residues 7–14 at the N-terminal heptad repeats of tropomyosin isoform 5. *Arch. Biochem. Biophys.* 378:16–24.

Watakabe, A., R. Kobayashi, and D. M. Helfman. 1996. N-tropomodulin: a novel isoform of tropomodulin identified as the major binding protein to brain tropomyosin. *J. Cell Sci.* 109:2299–2310.

Weber, A., C. R. Pennise, G. G. Babcock, and V. M. Fowler. 1994. Tropomodulin caps the pointed ends of actin filaments. *J. Cell Biol.* 127:1627–1635.

Weber, A., C. R. Pennise, and V. M. Fowler. 1999. Tropomodulin increases the critical concentration of barbed end-capped actin filaments by converting ADP.P(i)-actin to ADP-actin at all pointed filament ends. *J. Biol. Chem.* 274:34637–34645.

Yamaguchi, M., R. M. Robson, M. H. Stromer, D. S. Dahl, and T. Oda. 1982. Nemaline myopathy rod bodies: structure and composition. *J. Neurol. Sci.* 56:35–56.